THE AMERICAN SOCIETY OF MECHANICAL ENGINEERS
345 E. 47th St., New York, N.Y. 10017

INFLUENCE OF TURBULENCE PARAMETERS AT SUPPLY INLET ON ROOM AIR DIFFUSION

M.N.A. Saïd
Institute for Research in Construction
National Research Council
Ottawa, Ontario, Canada

D.B. Jouini and E.G. Plett
Mechanical and Aerospace Engineering Dept.
Carleton University
Ottawa, Ontario, Canada

ABSTRACT

Air flow conditions at the supply opening, which are used as boundary conditions in a numerical simulation, must be applied in order to proceed with the numerical solution of the air flow within a room. Among the conditions usually specified are the turbulence parameters, including the turbulence kinetic energy or the turbulence intensity and turbulent kinetic energy dissipation rate. Investigators have used a variety of expressions to estimate these quantities. A review of these expressions is presented in this paper. The focus of this paper is to assess the influence of prescribed turbulence intensity and turbulent kinetic energy dissipation rate at the supply diffuser on the computed air flow pattern, velocity, and turbulence intensity in the space served by the supply diffuser.

The study indicates that the computed results converge to values corresponding to the measured values at a relatively faster rate when lower values of the turbulence intensity are used at the inlet boundary conditions, but that the final converged solution does not seem to be influenced by the value of the turbulence intensity for the range studied (4% to 37.4%). Also, computed results do not seem to be affected by the value of the inlet dissipation rate of the turbulence kinetic energy used at the inlet boundary conditions. In the cases studied, grid effects were negligible.

NOMENCLATURE

A	area (m^2)
C_D	empirical constant
C_p	specific heat of air (J/kg-K)
D_h	hydraulic diameter (m)
g_i	gravitational acceleration in x_j direction (m/s^2)
h	width of the supply inlet diffuser (m) (Eqn. 11.)
H	room height (m)
I_o	turbulence intensity of the air at the supply diffuser.
k	turbulent kinetic energy (J/kg or m^2/s^2)
L	length of the room (Figure 1) (m)
L_D	characteristic length of the supply diffuser (m)
n	normal coordinate direction
P	pressure (Pa)
q	volumetric heat generation rate (W/m_3)
S_ϕ	dummy variable as defined in table 2
t	width/height of exit opening (Figure 1) (m)
u'	fluctuating velocity in x direction (m/s)
U_j	mean velocity in the x_j direction (m/s)
v_{rms}	root mean square velocity fluctuation (m/s) (Eqn. 15)
v'	fluctuating velocity in the y direction (m/s)
w'	fluctuating velocity in the z direction (m/s)
W	width of the room (m)
x_j	cartesian coordinate direction
x	horizontal distance from the wall where the supply diffuser is located (m)
α	thermal diffusivity of air (m^2/s)
β	coefficient of thermal expansion (1/K)
ε	dissipation rate of turbulent kinetic energy (J/kg-s)
ϕ	dummy variable as defined in Table 2
Γ	dummy variable as defined in Table 2
ℓ	length scale of turbulence (m)
λ	a constant in correlation Eqn (6)
ν	kinematic viscosity of air (m^2/s)
Θ	temperature difference (K)
ρ	air density
τ	time (s)

Subscripts

o	relating to the supply diffuser location conditions
e	relating to the exit diffuser conditions

Presented at the ASME Winter Annual Meeting
New Orleans, Louisiana — November 28—December 3, 1993

INTRODUCTION

Air flow conditions at the supply opening, which are used as boundary conditions in a numerical simulation, are known to have strong influence on the air flow pattern within the room (Nielsen, 1989). The size, type, and location of the air supply diffuser also influence computed thermal conditions and air movement in ventilated spaces (Mathisen, 1990; Chen et al., 1991; Chen and Jiang, 1992).

A uniform mean velocity and temperature distribution is usually assumed for the air flow coming from the supply diffuser. The turbulent kinetic energy, k, and its dissipation rate, ε, cannot be measured directly. Consequently, investigators have used a variety of expressions to compute these quantities from measurable quantities. Six of these relationships are reviewed in this paper, and are summarized in Table 1. The focus of this paper is to assess the influence of prescribed turbulence intensity (I_o) and turbulent kinetic energy dissipation rate at the supply diffuser (ε_o) on the computed air flow pattern, velocity, and turbulence intensity in the space served by the supply diffuser.

The turbulent kinetic energy (k_o) at the supply diffuser is commonly calculated by:

$$k_o = (3/2)I_o^2 U_o^2 \qquad (1)$$

where I_o is the turbulence intensity of the air at the supply diffuser. I_o is defined as:

$$I_o = u_o'/U_o \qquad (2)$$

For free shear flows, Launder (1990) defined the dissipation rate of turbulent kinetic energy (ε) in terms of k and the length scale of turbulence, ℓ, through:

$$\varepsilon = k^{3/2}/\ell \qquad (3)$$

Several variations of Equation (3) have been used to estimate ε_o of air at the air supply diffuser (Table 1). Nielsen (1990) recommended the form of Equation (3) to be used for estimating ε_o. The turbulent kinetic energy at the supply diffuser, k_o, is calculated by Equation (1) and the turbulence length scale, ℓ_o, is given in terms of the width of the inlet slot diffuser, h, by:

$$\ell_o = 0.1\ h \qquad (4)$$

Skovgaard and Lemaire (1990) recommended the following correlation:

$$\varepsilon_o = C_m^{3/4} k_o^{3/2}/\ell_o \qquad (5)$$

where $C_m = 0.09$ and $\ell_o = 0.03\ D_h$. D_h is the hydraulic diameter of the supply diffuser which is given by:

$$D_h = 4\ A_o\ /\ \text{supply diffuser perimeter},$$

where A_o is the cross-sectional area of the supply diffuser.

The form of Equation (5) is similar to that usually used to estimate ε at solid wall boundaries.

Awbi (1989) used:

$$\varepsilon_o = k_o^{3/2}/(\lambda H) \qquad (6)$$

Where λ is a constant taken as 0.005 and H is the room height or the square root of the cross-sectional area of the room. k_o is estimated by Equation (1) in which $I_o^2 = 0.14$ ($I_o = 37.4\%$). For $I_o = 4\%$ and H = room height, Awbi's correlation gives ε_o values close to that calculated through the correlation suggested by Nielsen 1990 (Equations (3) and (4)). For $I_o = 37.4\%$ ($I_o^2 = 0.14$), the calculated value of ε_o is three orders of magnitude higher than that for $I_o = 4\%$.

Murakami and Kato (1989) used the following correlation:

$$\varepsilon_o = C_D k_o^{3/2}/\ell_o \qquad (7)$$

where C_D is an empirical constant taken as 0.09, k_o=0.005 and ℓ_o= 0.33. The values of k_o and ℓ_o (both dimensionless) were obtained from measurements which were non-dimensionlized by the inlet velocity, U_o^2, and the width of the supply diffuser respectively. The suggested value of k_o, 0.005, corresponds to a turbulence intensity of 5.8%. The form of Equation (7) had also been suggested by Launder and Spalding (1974). Kurabuchi et al. (1990) also used the form of Equation (7). They recommended the following empirical values for k_o $(m/s)^2$ and ℓ_o (m):

for a straight duct end or for a nozzle type jet diffuser:

$$k_o = 0.01\ U_o^2 \text{ to } 0.03\ U_o^2 \qquad (8a)$$

$$\ell_o = 0.05\ L_D \text{ to } 0.25\ L_D, \qquad (8b)$$

for an "anemo type" radial diffuser:

$$k_o = 0.05\ U_o^2 \text{ to } 0.15\ U_o^2 \qquad (9a)$$

$$\ell_o = 0.01\ L_D \text{ to } 0.02\ L_D, \qquad (9b)$$

where U_o is the area averaged inflow velocity (m/s) and L_D (m) is the characteristic length of the supply diffuser. The recommended correlations for k_o in Equation (8a) corresponds to a turbulence intensity in the range 8% to 14% for a nozzle type jet diffuser, and in Equation (9a) to a range of 18% to 32% for a radial type diffuser. Using Equation (7), the suggested range for k_o and ℓ_o for a nozzle type jet diffuser, Equations (8a) and (8b), results in approximately the same value of ε_o as obtained from the correlations of Murakami and Kato (1989).

The form of Equation (7) was also used by Lamers and Velde (1989). They estimated the turbulence kinetic energy, k_o, from measured fluctuating velocity at the supply diffuser through:

$$k_o = (3/2)u_o'^2 \qquad (10)$$

where $u_o'=0.04U_o$, according to measurements by Nielsen et al.(1978).

Equation (10) is equivalent to a combination of Equations (1) and (2), expressed directly in terms of fluctuating velocity. U_o is the area averaged mean velocity at the supply diffuser. The expression given above corresponds to a turbulence intensity, u_o'/U_o, of 4%. Lamers and Velde deduced a relationship between the inlet mixing length, ℓ_o (m), and the width, h (m), of the inlet slot diffuser, as given by:

$$\ell_o = 0.1\ h/2 \qquad (11)$$

Values of ε_o computed using Equations (1) through (11) vary considerably depending on the correlation as well as the values of k_o and ℓ_o used. The objective of this study was to asses the influence of prescribed ε_o and turbulence intensity (I_o) at the supply diffuser on computed air flow patterns, velocity and turbulence intensity in ventilated spaces. As noted earlier, the effect of supply air momentum and temperature has been studied by others (e.g. Chen and Jiang, 1992 and Nielsen, 1979).

COMPUTER PROGRAM

The code EXACT3, developed by Kurabuchi et al. (1990) was used in this investigation. It is a three-dimensional finite difference computer program for simulating buoyant, turbulent air flows within buildings, using the Boussinesq approximation in accounting for buoyancy effects, and the high-Reynolds-number k-ε turbulence closure approach. It employs a staggered grid and a hybrid upwind/central differencing combination scheme for the numerical solution. The governing equations can be written in the general elliptic form for an incompressible fluid as:

$$\partial\phi/\partial\tau + \partial(U_j\phi)/\partial x_j - \partial(\Gamma_\phi\partial\phi/\partial x_j)/\partial x_j = S_\phi \qquad (12)$$

where the parameters ϕ, Γ_ϕ and S_ϕ are identified for each equation in Table 2. Wall boundary conditions used by EXACT3 are also listed in Table 2.

A pressure relaxation method is used to satisfy the Poisson equation for mass conservation. The governing equations are solved by an explicit time marching technique using the marker and cell method (Harlow and Welch, 1965). The solution time step was chosen to ensure stability. Although the solution does involve the solution of a nonsteady equation (12), since the k-ε model is used, which is already a time averaged model for turbulence, the solutions leading to the final converged solution are not true time-wise solutions. Consequently, the steps leading to the final 'steady' solution are referred to as iterations, and the final solution is the converged solution when residuals, based on changes between subsequent iterations, are considered to be sufficiently small.

SIMULATION METHOD

The simulation test case described by Nielsen (1990) was selected as the benchmark for this study because reliable measured data are available for this case. This test case has been used for evaluating various computational fluid dynamics codes within the frame work of the International Energy Agency Annex 20 (Lemaire, 1992).

Figure 1 shows the configuration of the room used in the simulations. The room is equipped with a slot supply air diffuser and a slot exhaust opening. The length of both slots is equal to the width of the room. Thus the air flow within the room, especially in the region of the midpoint along the length of the slot diffusers, is approximately two dimensional. The symmetry assumption was used and half the room domain was simulated using a non-uniform grid of 37 x 34 x 15, as illustrated in Fig. 2a, with some studies to examine the effect of grid size conducted with a 60 x 60 x 15 grid, as illustrated in Fig. 2b. Isothermal conditions were assumed throughout. The computation of all cases was started with guessed fields as initial conditions for all variables as specified in EXACT3. The changing values of residuals with number of iterations are given in Table 3, for momentum, k and ε residuals. Since all three of these residuals are reducing with increasing numbers of iterations, it may not matter which is chosen to use as the basis for deciding on whether or not the solution had converged. In the present case, the momentum residual was used. The solution was judged to have converged when there are no noticeable changes in the first two significant figures of the volumetric root mean square (rms) residual of the momentum equation (Kurabuchi et al., 1990) for about 100 iterations. At the point where the solution was accepted to have converged, the volumetric rms residual of the momentum equation was 2.2×10^{-4}. The computations were performed on an IBM 3090 main frame computer system.

Inlet Boundary Conditions

The air velocity in the X-direction, (Fig. 1) U_o, at the supply air diffuser was set to 0.455 m/s. The lateral velocity components, V_o and W_o, were set to zero. This corresponds to a supply air flow rate of 0.229 m^3/s (air density was assumed to be 1.2 kg/m^3) and a supply Reynolds number, Re_o, of 5000 where Re_o was defined as:

$$Re_o = U_o h/\nu \qquad (13)$$

where ν is the kinematic viscosity of the air.

Specification of the turbulent kinetic energy, k_o, and its dissipation rate, ε_o, at the supply air diffuser is described later.

Exit Air Boundary Conditions

The normal velocity component at the exit, U_e, was derived from the continuity equation:

$$U_o = A_o U_o/A_o \quad (14)$$

and the other velocity components, pressure, and normal gradients ($\partial/\partial x$) of k_o and ε_o were assumed to be zero. A uniform distribution of variables was also assumed over the exit area.

RESULTS

Two grid distributions were examined for selected cases to examine the extent to which the solution might be grid dependent. The overall objective was to examine the effect of inlet turbulent kinetic energy, k_o, and inlet turbulent kinetic energy dissipation rate, ε_o, on the final converged solution. The effect of these will be discussed next, followed by a brief discussion of the effect of grid size and distribution.

Effect Of Inlet Turbulent Kinetic Energy (k_o)

To assess the influence of prescribed turbulent kinetic energy, k_o, at the supply air diffuser on room air diffusion, computations were conducted for four values of k_o. These were calculated using Equation (1) and turbulence intensities of 4%, 9%, 14% and 37.4%. The values 4% and 14% represent those most commonly used in work reported in the literature, and the 37.4% represents an extreme value in the literature. The 9% value is based on measurements by Jouini (1992) for an air-light fixture slot diffuser. In these computations ε_o was estimated using the correlation given by Equations (3) and (4).

The turbulence intensity results are presented in terms of the root mean square (rms) of the velocity fluctuation (v_{rms} (or simply rms in the figures) = $\sqrt{u'^2}$) calculated as:

$$v_{rms} = 0.91\sqrt{k} \quad (15)$$

Equation (15) is based on the assumption that $v'^2 = 0.6\ u'^2$, $w'^2 = 0.8\ u'^2$, and $k = 0.5\ (u'^2 + v'^2 + w'^2)$ (Nielsen, 1990).

Figures 3 to 5 show the vertical distribution of computed mean and rms velocity at x/H = 1 and x/H = 2, for various values of I_o and at different stages of the solution. The measured profiles by Nielsen et al. (1978) are also shown in these figures. These measurements were taken using a Laser-Doppler Anemometer and a scale model (Re=5000, H=89.3 mm, L/H=3.0, W/H=1.0, h/H=0.056, and t/H=0.16; see Figure 1 for notation). At early stages of the solution, Figures 3 and 4, computed results in the zone close to the wall jet region at the ceiling, x/H = 1.0, converge to values corresponding to the measured values at a relatively faster rate when lower values of the turbulence intensity are used at the inlet boundary conditions. However, the final converged solution, Figure 5, does not seem to be influenced by the value of the turbulence intensity used. Table 4 shows the effect of prescribed I_o (and also ε_o) on computation time. Computation time for the base-case (I_o = 4% and ε_o is estimated as per Nielsen, 1990) was 504 CPU minutes. As can be seen from Table 4, computation time increased by about 5% when I_o = 37.4% is used, as compared with values of around 4%.

As can be noted from Figures 3 and 4 for x/H = 2, at early stages of the solution, the momentum diffusion is slow in reaching locations further down stream from the inlet diffuser zone. This should be taken into considerations when selecting the monitoring point for the progress of the solution.

Effect of inlet turbulent kinetic energy dissipation rate (ε_o)

To isolate the effect of ε_o on computed room air diffusion, computations were conducted for the same value of k_o which was calculated using Equation (1) and a turbulence intensity of 4%. Three values of ε_o were considered which were calculated by the correlations suggested by Nielsen (1990), Skovgaard and Lemaire (1990), and Lamers and Velde (1989). For the same value of k_o, The value of ε_o calculated by the Nielsen correlation represented the upper limit which was about 5.5 times the value calculated by Lamers and Velde correlation. The value of ε_o calculated by the Skovgaard and Lemaire correlation was slightly higher (about 1.6 times) than that calculated by the Lamers and Velde correlation. Computed results for mean and rms velocity (Figures 6 to 8) do not seem to be affected by the value of ε_o used at the inlet boundary conditions. Computation time, however, was slightly decreased by about 1.3% when ε_o is estimated as suggested by Lamers and Velde (1989).

Figures 9 and 10 show the velocity distribution in the symmetry plane for I_o = 4% and 37.4%, and corresponding ε_o values estimated by the methods of Nielsen (1990) and Lamers and Velde (1989). Figure 9 shows the velocity distribution at an early stage of the solution (4000 iterations) whereas Figure 10 shows the results at the final converged state (35,415 iterations). As can be seen from these figures, the air circulation pattern does not seem to be influenced by either the value of the inlet turbulence intensity or the value of the inlet dissipation rate of the turbulence kinetic energy. The growth of the air supply jet near the ceiling is the same for all values of I_o and ε_o. The location of the centre of the circulation vortex is also the same for all values of I_o and ε_o

Effect of Number of Grid Points

A series of computer runs was made with the 60 x 60 x 15 grid to compare results for one case with those obtained with the 37 x 34 x 15 grid system, both of which are shown in Figure 2. The comparison of the computed mean and fluctuating velocities at two axial locations, after 25000 iterations, is shown in Figure 11. Although there are very slight differences in the results compared in this series of graphs, the differences are of the same order of magnitude as obtained with the variation in relational representation of k and ε for the models investigated. That is, at or approaching the final converged value, the two grids investigated gave essentially the same result.

CONCLUSIONS

Results of the study indicate that the computed results converge to values corresponding to the measured values at a relatively faster rate when lower values of the turbulence intensity are used at the inlet boundary conditions, but that the final converged solution does not seem to be influenced by the value of the turbulence intensity for the range studied (I_o =4% to 37.4%). Also, computed results do not seem to be affected by the value of the inlet dissipation rate of the turbulence kinetic energy used at the inlet boundary conditions. The momentum diffusion is slow in reaching locations down stream from the inlet diffuser zone. Consequently, in a solution such as this, it is important to monitor the changes taking place throughout the room before accepting the solution as having converged.

REFERENCES

Awbi, H.B. 1989, "Application of Computational Fluid Dynamics in Room Ventilation," Building and Environment, Vol. 24, No. 1, pp.73-84.

Chen, Q. and Jiang Z. 1992, "Air Supply Method and Indoor Environment," Indoor Environment, Vol. 1, No. 2, pp.88-102.

Chen, Q., Suter, P., and Moser, A. 1991, "Influence of Air Supply Parameters on Indoor Air Diffusion," Building and Environment, Vol. 26, pp.417-431

Harlow, F.H. and Welch, J.E. 1965, "Numerical Calculation of Time-Dependent Viscous Incompressible Flow of Fluid with Free Surface," The Physics of Fluids, Volume 8, No. 12, December, pp. 2182-2189.

Jouini, D.B. 1992, "Experimental Investigation of the Flow Properties in a Typical Office Space," M.Eng. Thesis, Carleton University, Ottawa, Ontario, Canada, June.

Kurabuchi, T., Fang, J. B., and Grot, R.A. 1990, "A Numerical Method for Calculating Indoor Airflows Using a Turbulence Model," National Institute of Standards and Technology, Gaithersburg, MD 20899, USA, Report No. NISTIR 89-4211, January.

Lemaire, A.D., Editor (in print 1992), "Room Air and Contaminant Flow - Evaluation of Computational Methods," Energy Conservation in Buildings and Community Systems Programme, International Energy Agency, Annex 20, Subtask-1 Summary Report.

Lamers, A.P.G.G. and Velde, R. van de. 1989, "Air Flow Patterns in Ventilated Rooms," Phoenics Journal, Vol 2, No. 2, pp. 219-238.

Launder, B.E. 1990, "An Introduction to Turbulence Modelling," IBM CFD Short Course Notes, Volume II, Fort Lauderdale, Florida, USA, May 14-18.

Launder, B.E. and Spalding, D.B. 1974, "The Numerical Computation of Turbulent Flows," Computer Methods in Applied Mechanics and Engineering, Vol. 3, pp. 269-289.

Mathisen, H.M. 1990, "Displacement Ventilation - The Influence of the Characteristics of the Supply Air Terminal Device on the Air Flow Pattern," Indoor Air, Vol. 0, pp. 3-20.

Murakami, S. and Kato, S. 1989, "Numerical and Experimental Study on Room Airflow - 3-D Predictions Using the k-ε Model," Building and Environment, Vol. 24, No. 1, pp. 85-97

Nielsen, P.V., Restivo, A. and Whitelaw, J.H. 1978, "The velocity characteristics of ventilated rooms," Transactions of the ASME, J. of Fluids Engineering, Vol. 100, September, pp. 291-298.

Nielsen, P.V., Restivo, A. and Whitelaw, J.H. 1979, "Buoyancy-Affected Flows in Ventilated Rooms," Numerical Heat Transfer , Vol. 2, pp. 115-127.

Nielsen, P.V. 1989, "Airflow Simulation Techniques - Progress and Trends," Proc 10th AIVC Conference, Espoo, Finland, September 25-28, 1989.

Nielsen, P.V. 1990, "Specification of A Two-Dimensional Test Case," International Energy Agency Annex 20, Research Item 1.45 Technical Report, Aalborg University, Aalborg, Denmark, ISSN 0902-7513 R9040, November.

Skovgaard, M. and Lemaire, A.D. 1990, "Basic Model," Technical Note on Research Item 1.11 "Representation of Boundary Conditions at Supply Opening", International Energy Agency Annex 20, TNO, Delft, The Netherlands February.

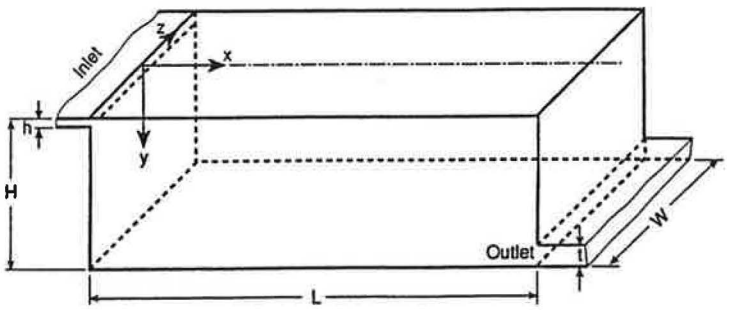

Figure 1. GEOMETRY AND COORDINATE SYSTEM:
H = 3.0; L/H = 3.0; W/H = 1.0;
h/H = 0.056; t/H = 0.16

Table 1. SUMMARY OF CORRELATIONS FOR ESTIMATING ε_o

Source	Formula	Parameters
Awbi, 1989	$\varepsilon_o = k_o^{3/2}/(\lambda H)$	$\lambda = 0.005$ $k_o = (3/2) I_o^2 U_o^2$ H: room height or square root of cross-sectional area of room
Kurabuchi et al., 1990	$\varepsilon_o = C_D k_o^{3/2}/(\ell_o)$	For duct end, or for a nozzle type diffuser: $k_o = 0.01\ U_o^2$ to $0.03\ U_o^2$ $\ell_o = 0.05\ L_D$ to $0.25\ L_D$ For an "anemo" type radial diffuser: $k_o = 0.05\ U_o^2$ to $0.15\ U_o^2$ $\ell_o = 0.01\ L_D$ to $0.02\ L_D$ L_D = inlet representative length scale $C_D = 0.09$
Lamers & Velde, 1989	$\varepsilon_o = C_\mu k_o^{3/2}/\ell_o$	$k_o = (3/2) u_o'^2$ u_o'= measured fluctuating Velocity, $= 0.04\ U_o$ $\ell_o = 0.1\ h/2$ h = width of inlet slot diffuser $C_\mu = 0.09$
Murakami & Kato, 1989	$\varepsilon_o = C_D k_o^{3/2}/\ell_o$	$k_o = 0.005$ $\ell_o = 0.33$ $C_D = 0.09$
Nielsen, 1990	$\varepsilon_o = k_o^{3/2}/\ell_o$	$k_o = (3/2) I_o^2 U_o^2$ $I_o = 0.04$ $\ell_o = 0.1\ h$ h: width of inlet slot diffuser
Skovgaard & Lemaire, 1990	$\varepsilon_o = (C_\mu)^{3/4} k_o^{3/2}/\ell_o$	$k_o = (3/2) I_o^2 U_o^2$ $I_o = 0.04$ $\ell_o = 0.03\ D_h$ $C_\mu = 0.09$ D_h: hydraulic diameter of inlet diffuser

Table 2. VALUES OF ϕ, Γ_ϕ AND S_ϕ ASSOCIATED WITH EQUATION (12)

ϕ	Γ_ϕ	S_ϕ
1	0	0 (Continuity)
U_i	$\nu + \nu_t$	$(-1/\rho)\partial P/\partial x_j - \beta g_i \Theta$
Θ	$\alpha + \nu_t/\sigma_\Theta$	$q/\rho c_p$
k	$\nu + \nu_t/\sigma_k$	$\nu_t + G - \varepsilon$
ε	$\nu + \nu_t/\sigma_\varepsilon$	$(C_1\nu_t S - C_2\varepsilon + C_3 G)\varepsilon/k$

$\nu_t = C_\mu k^2/\varepsilon$, eddy viscosity

$S = (\partial U_i/\partial x_j - \partial U_j/\partial x_j)\partial U_i/\partial x_j$

$G = \beta g_i(\nu_t/\sigma_\Theta)\partial\Theta/\partial x_i$

Empirical coefficients:

$C_\mu = 0.09$, $C_1 = 1.44$, $C_2 = 1.92$, $C_3 = 1.0$,
$\sigma_k = 1.0$, $\sigma_\varepsilon = 1.3$, $\sigma_\Theta = 0.9$

Wall Boundary Conditions:

$U_n = 0.0$
$U_t \propto y^{1/7}$, where y is distance from wall
$\partial k/\partial n = 0.0$
$\varepsilon = (C_\mu)^{3/4}k^{3/2}/Z$, where Z is the distance from wall surface to centre of the fluid cell immediately adjacent to wall

Table 3. RESIDUAL CHANGE WITH NUMBER OF ITERATIONS FOR THE BASE CASE - NIELSEN 1990

Number of Iterations	Momentum Residual	k Residual	ε Residual
4,000.	0.00391	$0.12(10^{-3})$	$0.18(10^{-4})$
8,000.	0.00248	$0.82(10^{-4})$	$0.53(10^{-5})$
13,000.	0.00203	$0.72(10^{-4})$	$0.31(10^{-5})$
25,000.	0.00038	$0.23(10^{-4})$	$0.90(10^{-6})$
35,415.	0.00022	$0.12(10^{-4})$	$0.24(10^{-6})$

Table 4. EFFECT OF PRESCRIBED I_o AND ε_o ON COMPUTATION TIME

I_o	ε_o	Computation Time relative to base-case
4%	Nielsen, 1990	100% (base-case*)
9%	Nielsen, 1990	101.3%
14%	Nielsen, 1990	102.2%
37.4%	Nielsen, 1990	105.2%
4%	Lamers & Velde, 1989	98.7%

* computation time = 504 CPU minutes

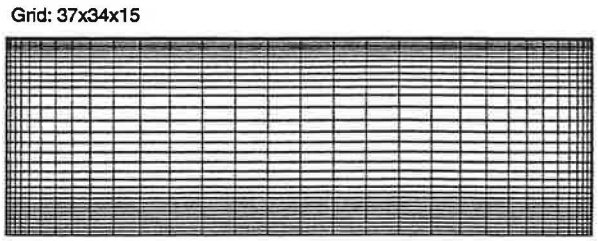

Figure 2a. GRID OF 37 x 34 x 15 AS USED FOR MOST OF THE COMPUTATIONS

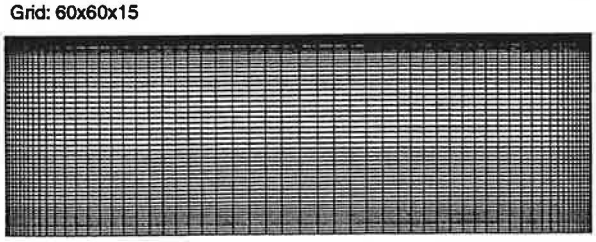

Figure 2b. GRID OF 60 x 60 x 15 AS USED FOR SOME OF THE COMPUTATIONS FOR COMPARISONS

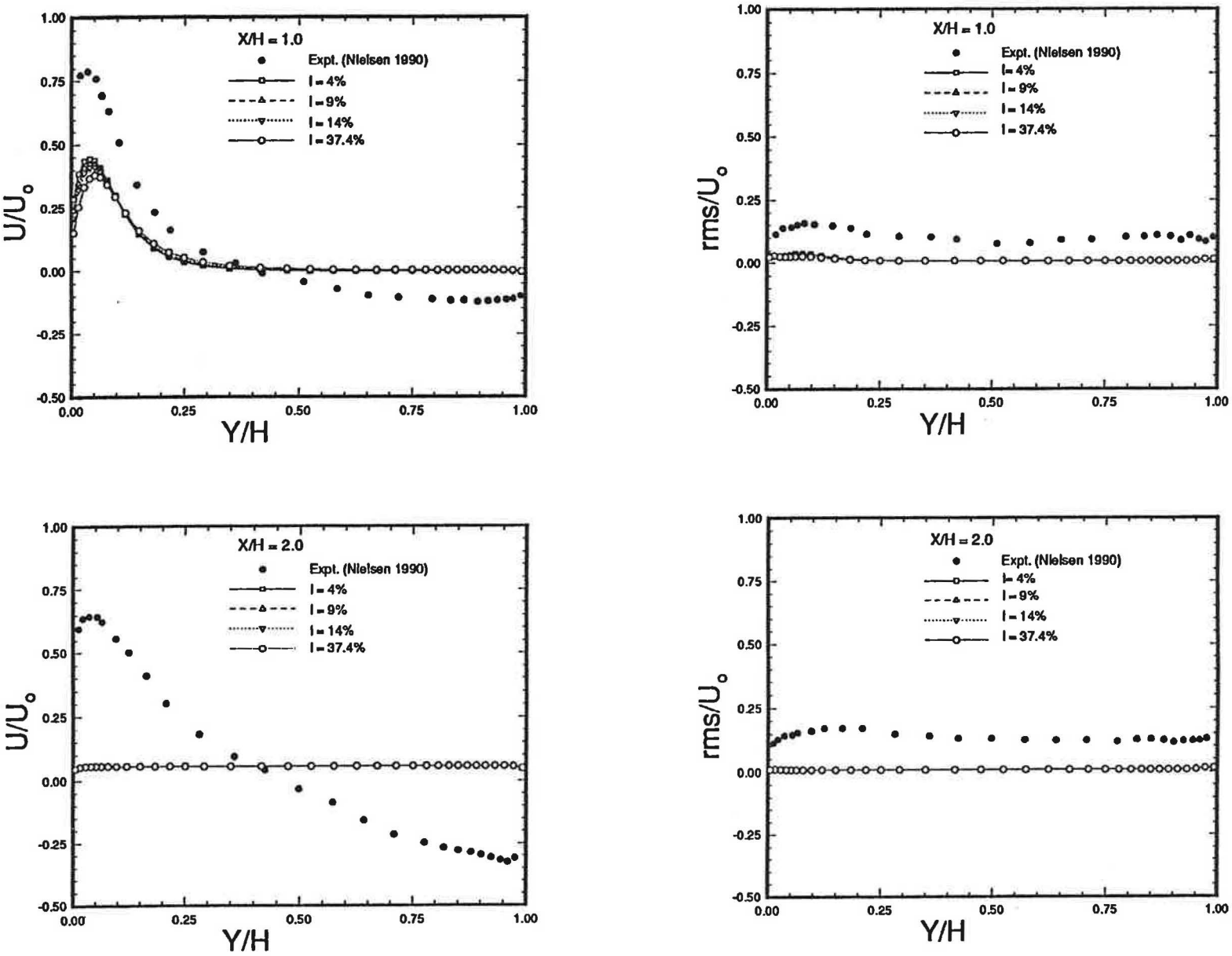

Figure 3. EFFECT OF I_o ON COMPUTED MEAN AND RMS VELOCITY AFTER 4,000 ITERATION STEPS

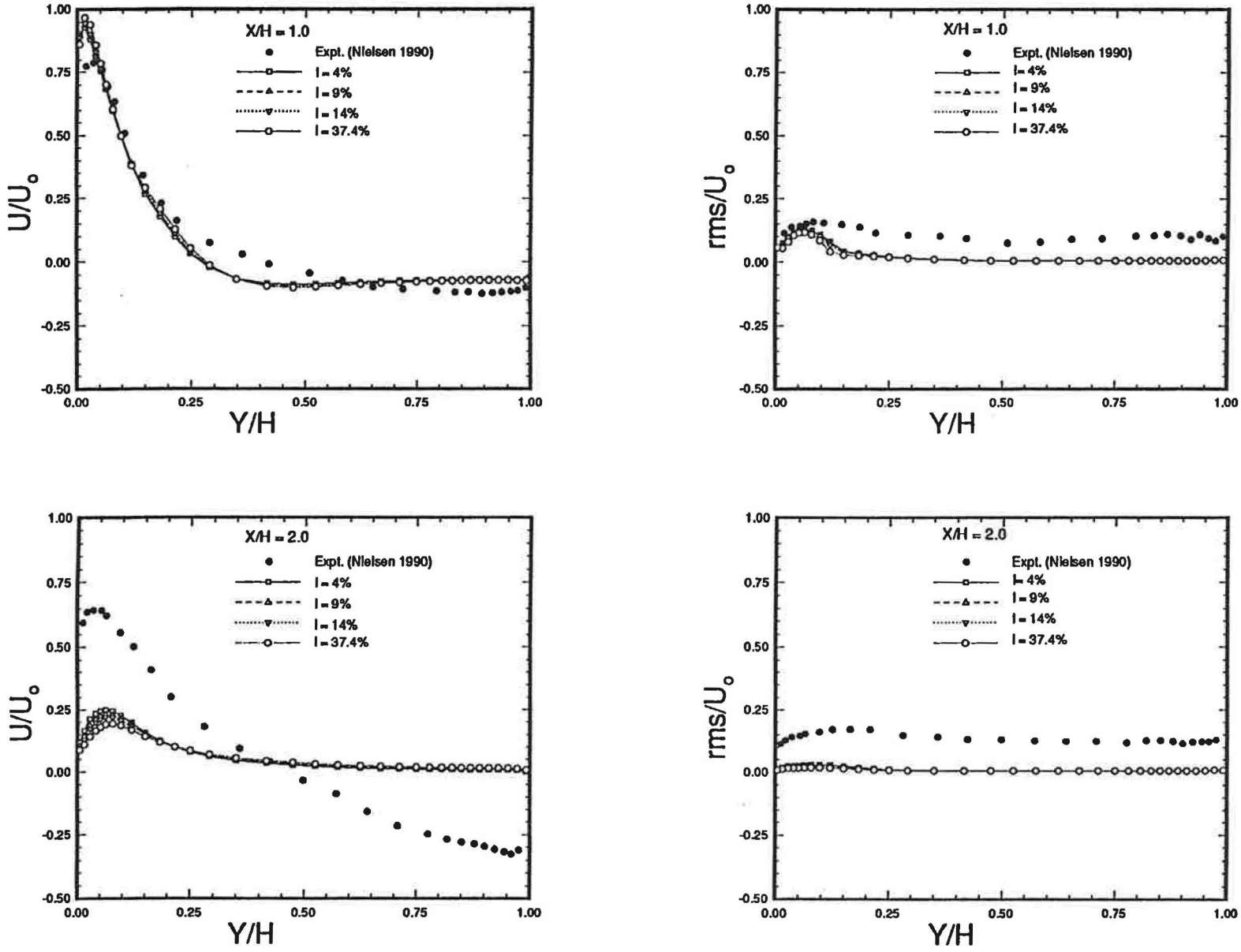

Figure 4. EFFECT OF I_o ON COMPUTED MEAN AND RMS VELOCITY AFTER 8,000 ITERATION STEPS

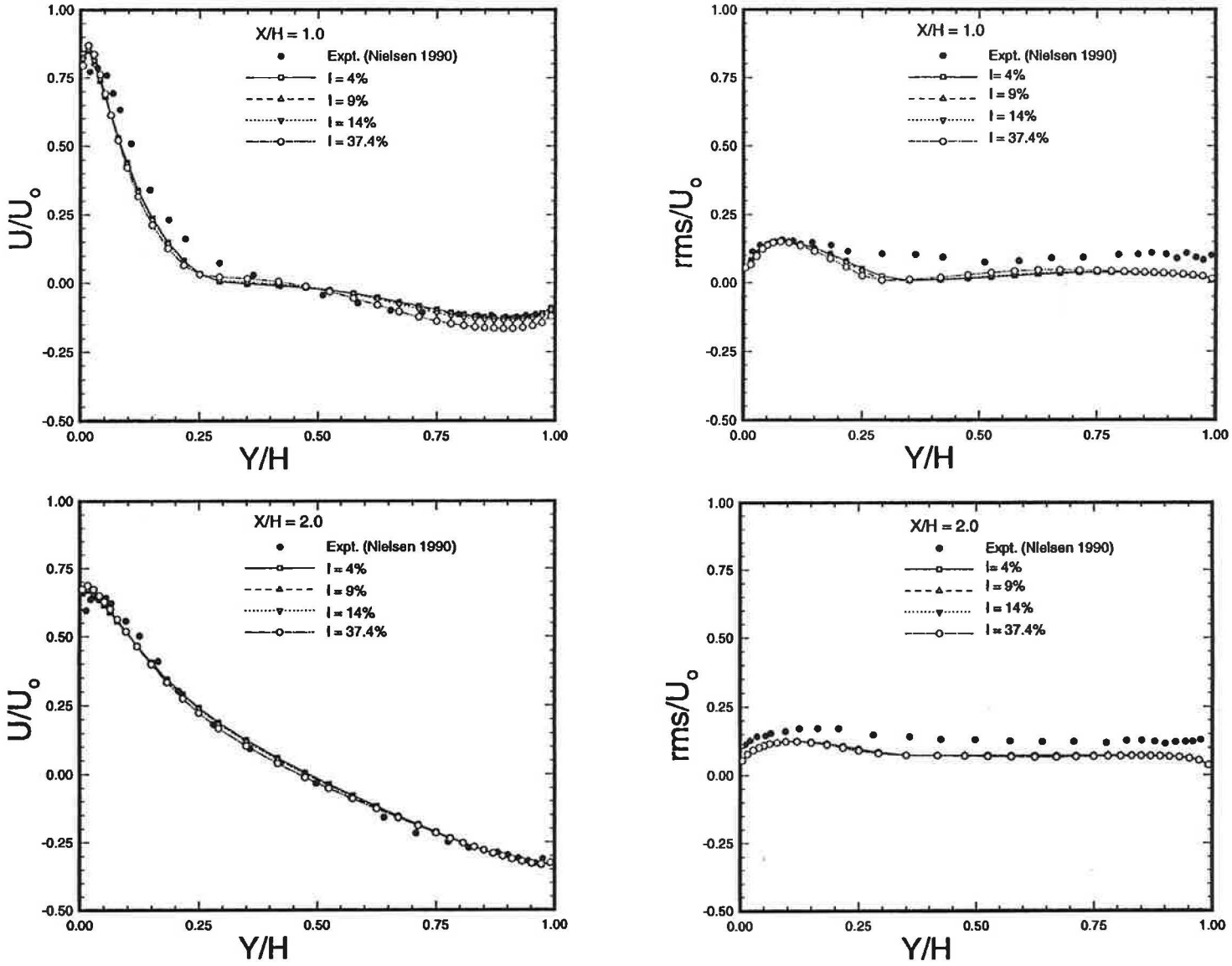

Figure 5. EFFECT OF I_o ON COMPUTED MEAN AND RMS VELOCITY FOR THE FINAL CONVERGED SOLUTION, AFTER 35,415 ITERATION STEPS

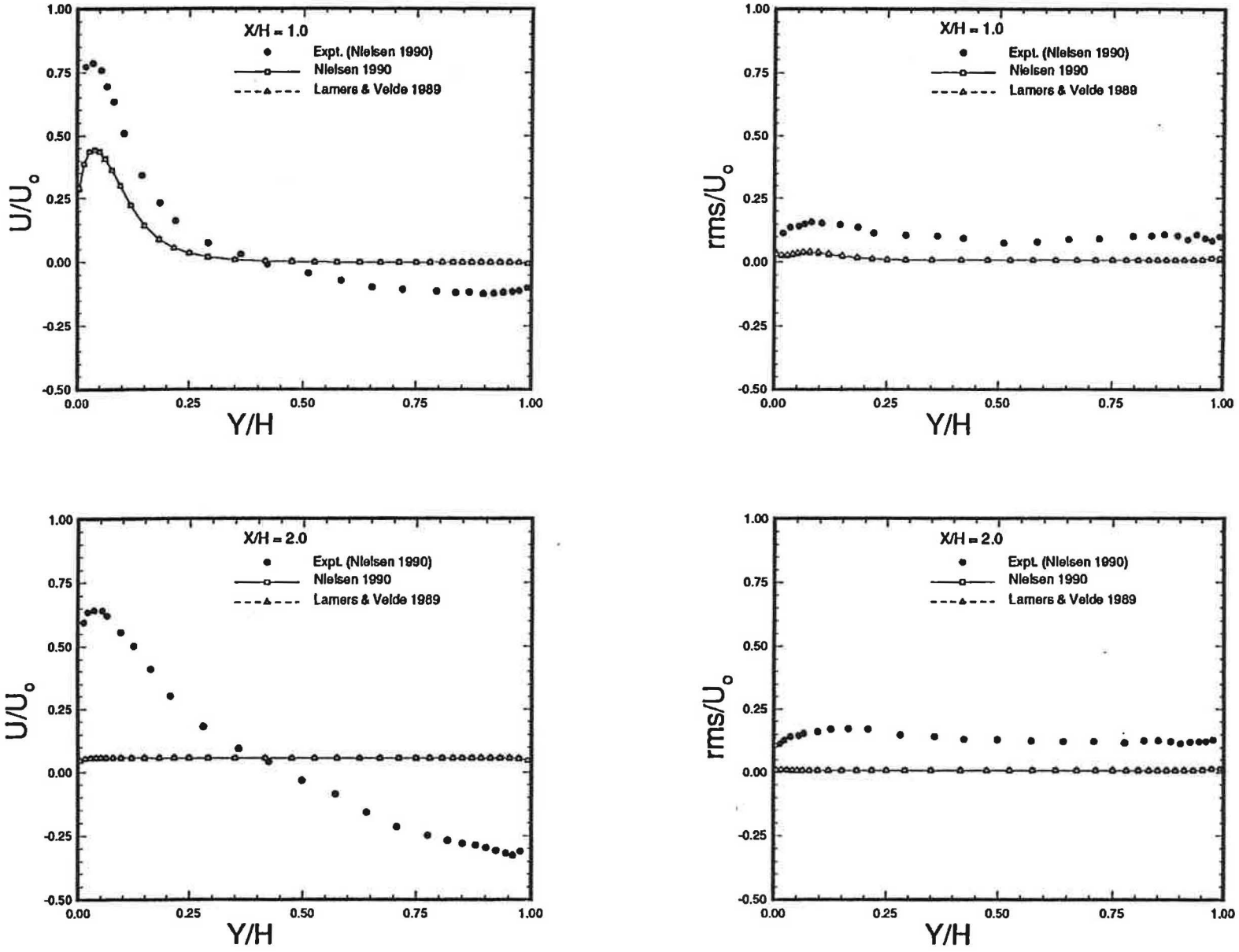

Figure 6. EFFECT OF ε_o ON COMPUTED MEAN AND RMS VELOCITY AFTER 4,000 ITERATION STEPS

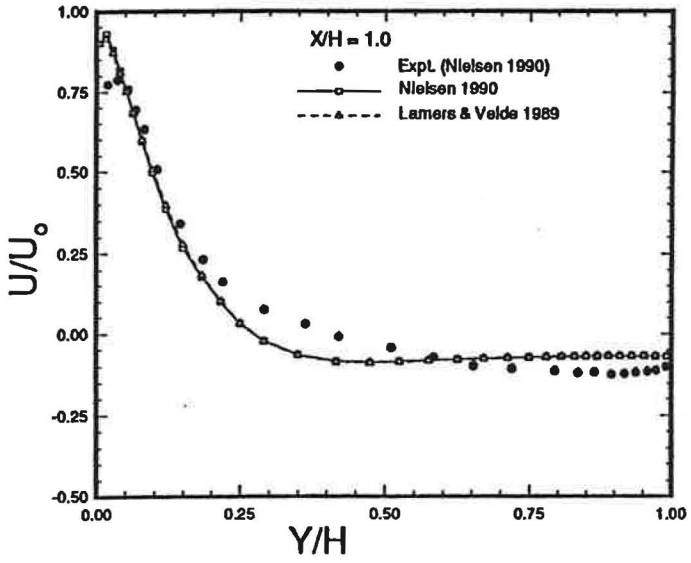

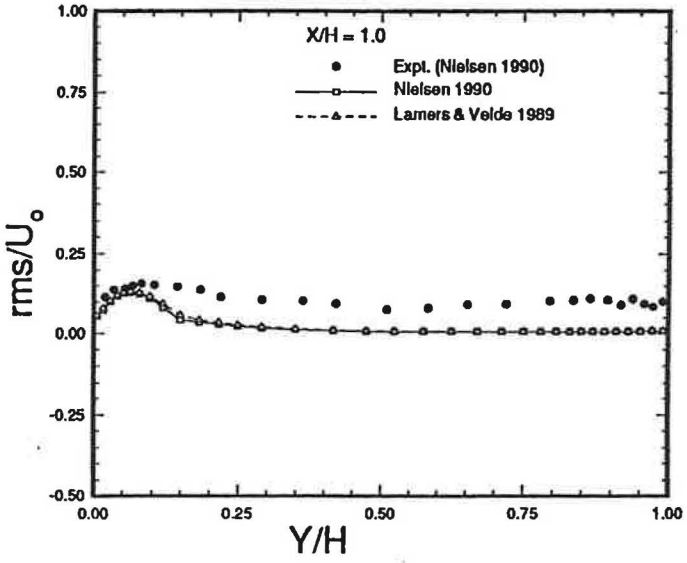

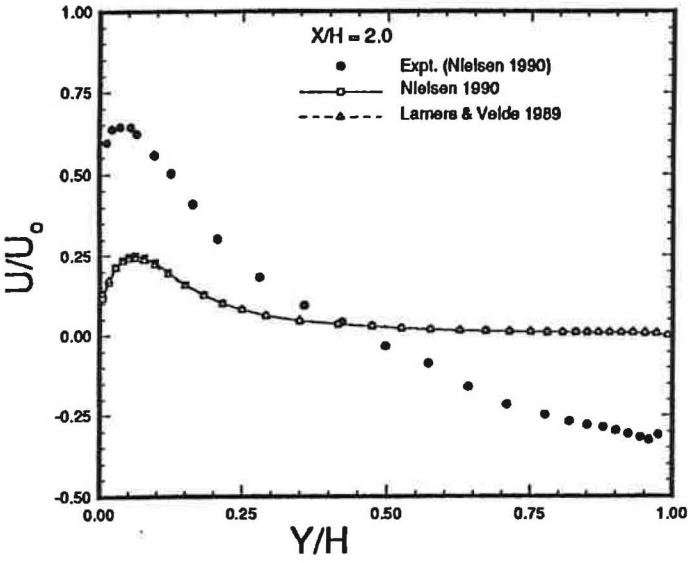

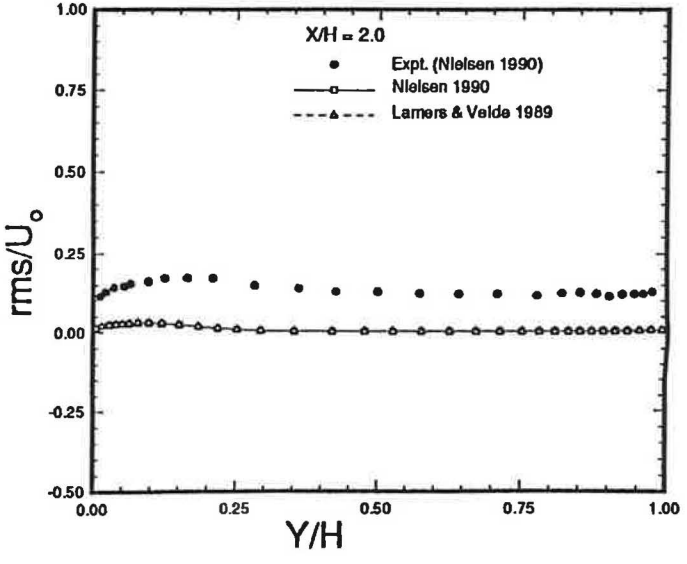

Figure 7. EFFECT OF ε_o ON COMPUTED MEAN AND RMS VELOCITY AFTER 8,000 ITERATION STEPS

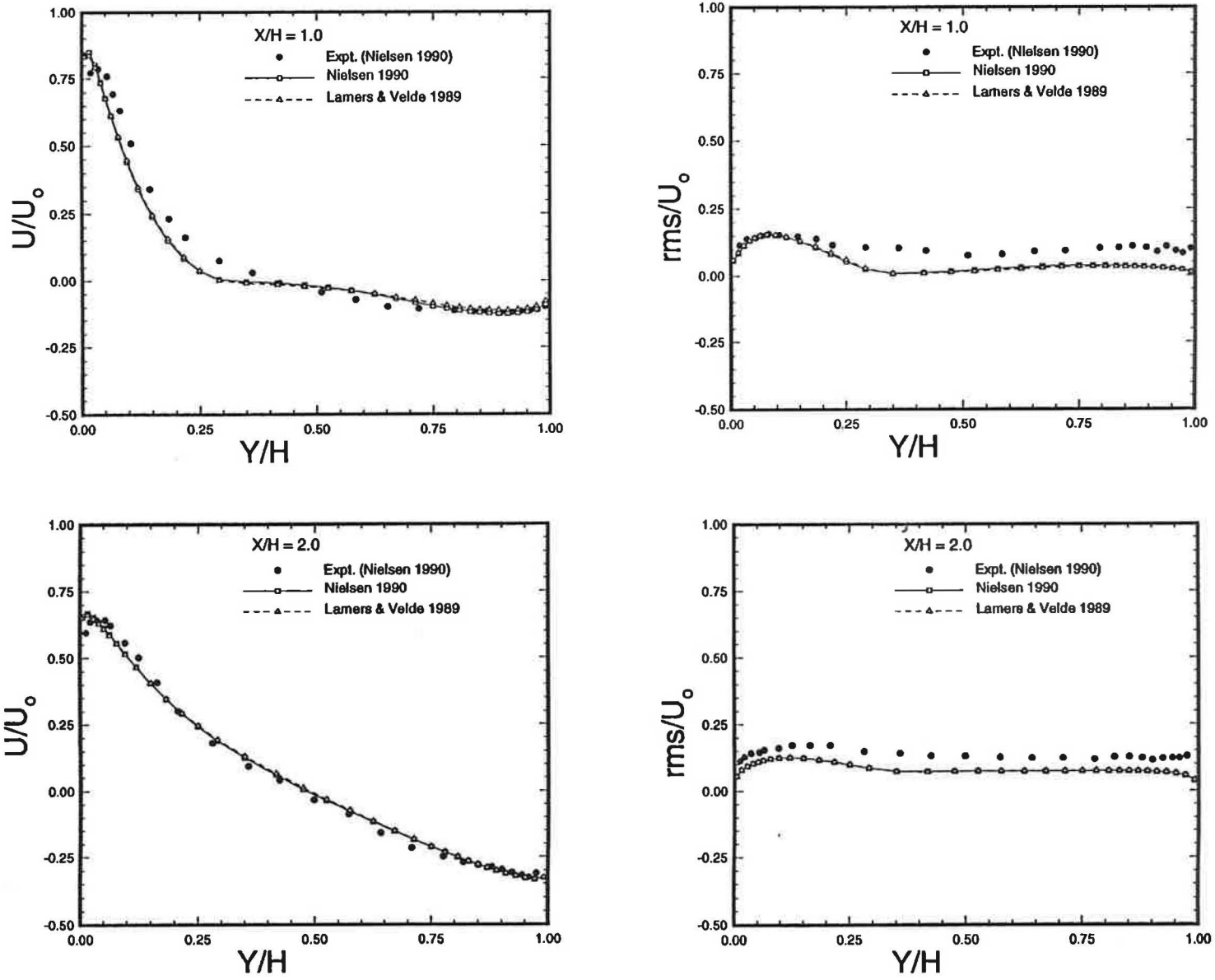

Figure 8. EFFECT OF ε_o ON COMPUTED MEAN AND RMS VELOCITY FOR THE FINAL CONVERGED SOLUTION, AFTER 35,415 ITERATION STEPS

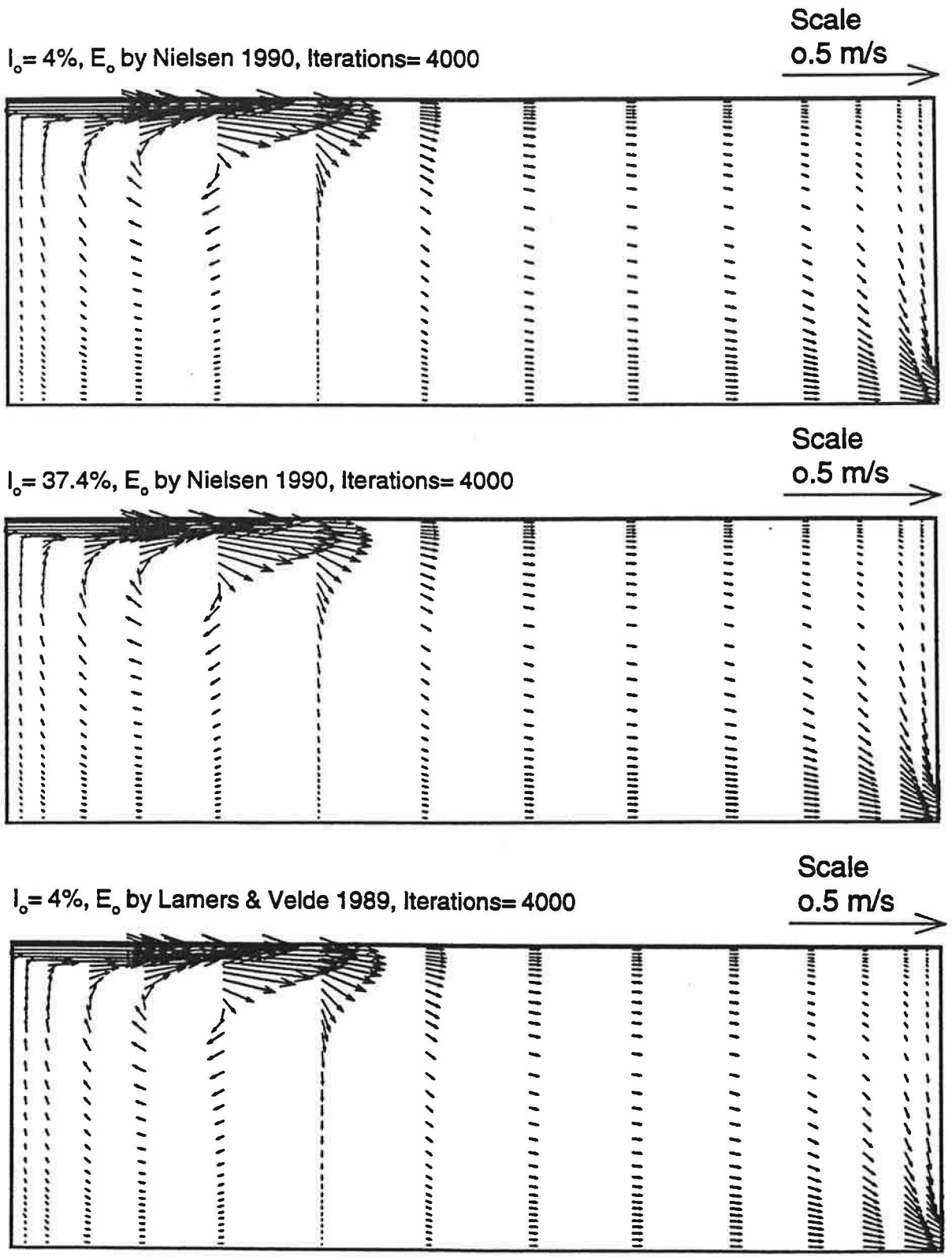

Figure 9. VELOCITY DISTRIBUTION IN THE SYMMETRY PLANE - EFFECT OF I_o AND ε_o ON COMPUTED MEAN AND RMS VELOCITY AFTER 4,000 ITERATION STEPS

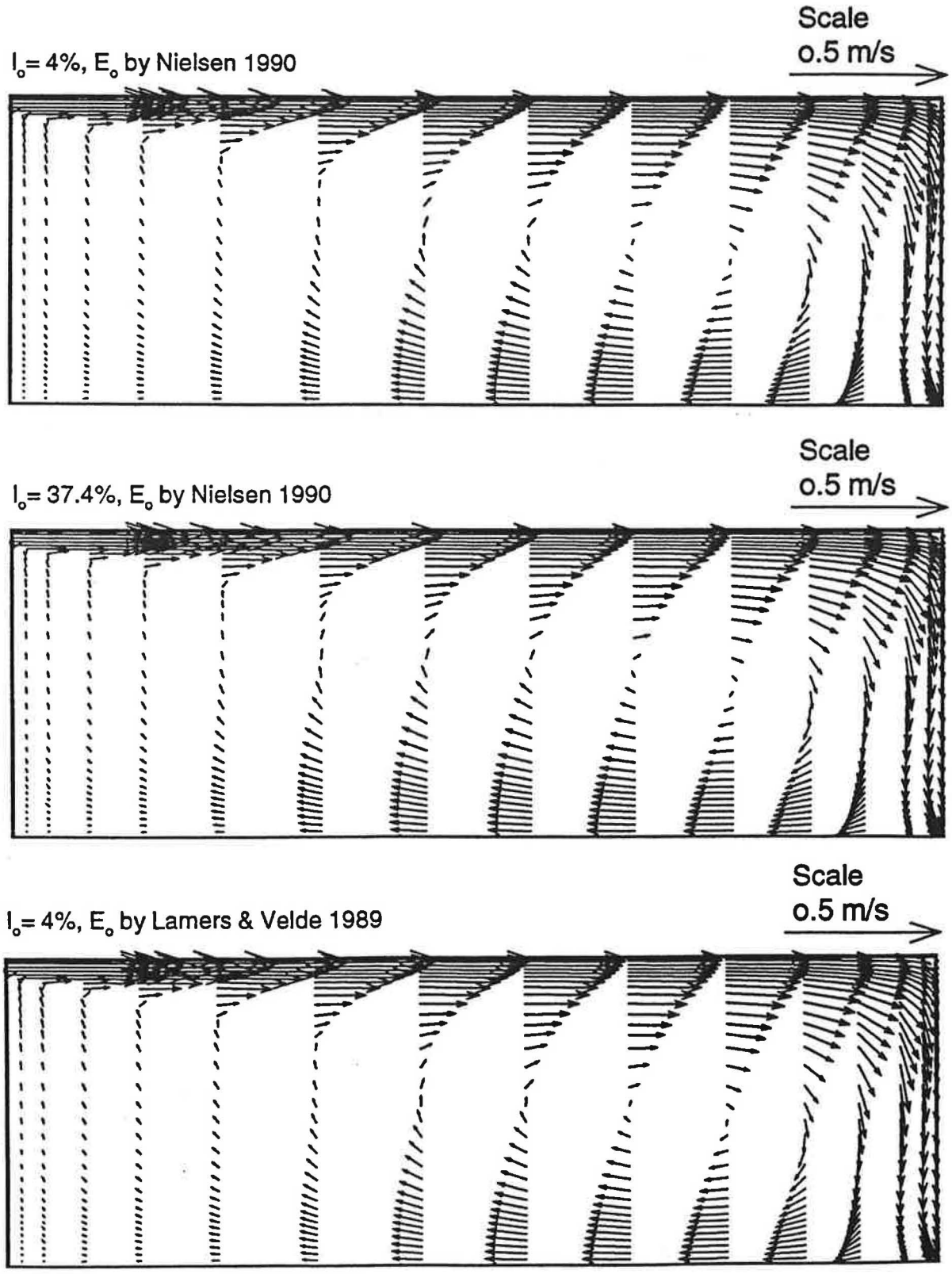

Figure 10. VELOCITY DISTRIBUTION IN THE SYMMETRY PLANE - EFFECT OF I_o AND ε_o ON COMPUTED MEAN AND RMS VELOCITY AT THE FINAL CONVERGED SOLUTION, AFTER 35,415 ITERATION STEPS

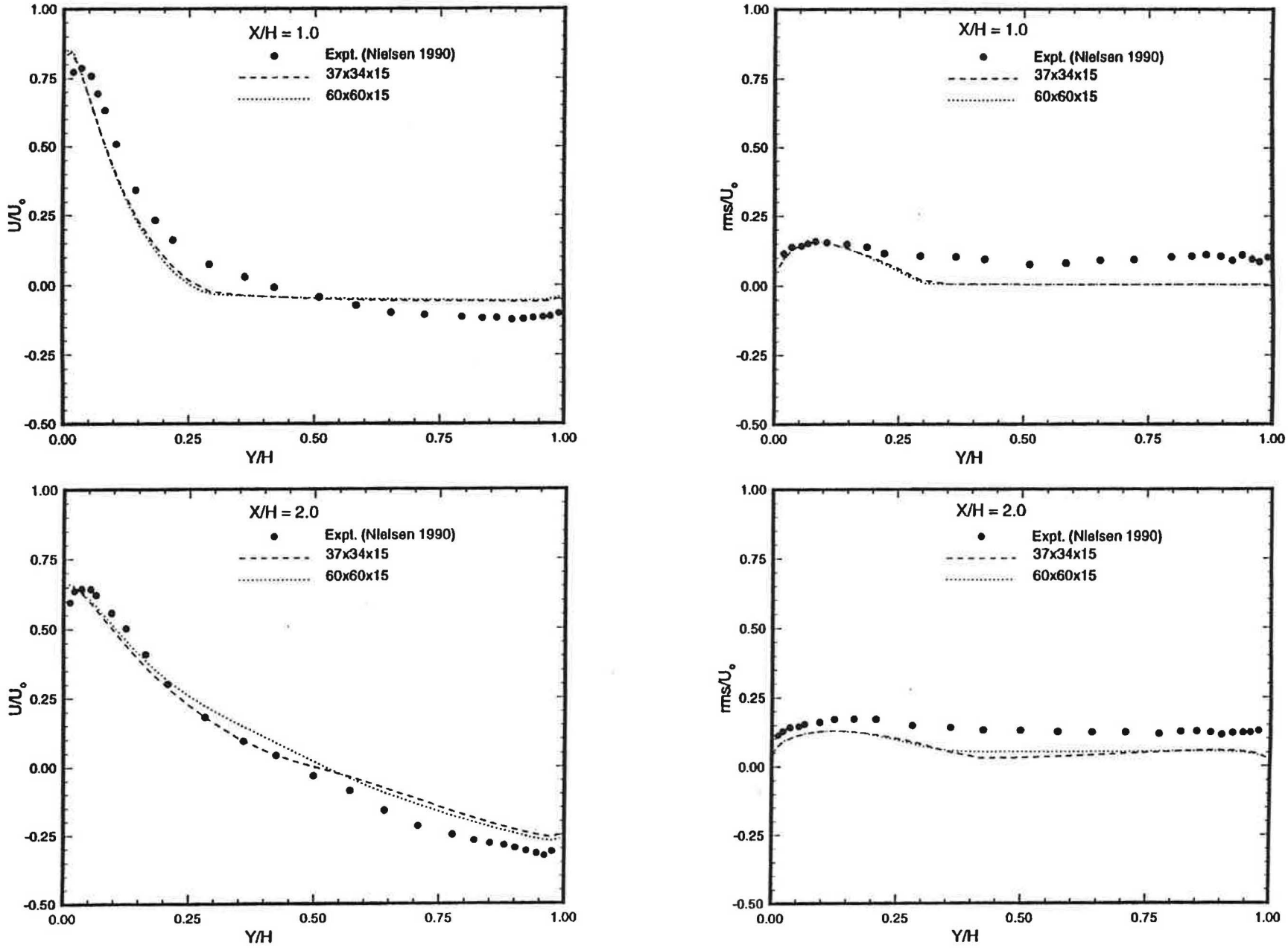

Figure 11. EFFECT OF GRIDING ON COMPUTED MEAN AND RMS VELOCITY AFTER 25,000 ITERATION STEPS, FOR THE TWO GRID SYSTEMS SHOWN IN FIGURE 2.